STATISTICS, OPTIMIZATION AND INFORMATION COMPUTING
Stat., Optim. Inf. Comput., Vol. **14**, August 2025, pp 469–485.
Published online in International Academic Press (www.IAPress.org)

Convergence of the Error in Hanafi-Wold's Procedure on the PLS-PM Task

Abderrahim Sahli [1,*], Zouhair El Hadri [1], Mohamed Hanafi [2]

[1]*Mathematics, Statistics, and Applications Laboratory, Faculty of sciences, Mohammed V University in Rabat, Morocco*
[2]*Research unit in Statistics, Sensometrics and Chemometrics, Oniris VetAgroBio, Nantes, France*

Abstract Partial least squares path modeling is a statistical method that facilitates examining intricate dependence relationships among various blocks of observed variables, each characterized by a latent variable. The computation of latent variable scores is a pivotal step in this method and it is accomplished through an iterative procedure. Within this paper, we investigate and tackle convergence challenges related to Hanafi-Wold's procedure in computing components for the PLS-PM algorithm. Hanafi-Wold's procedure, as well as alternative procedure, demonstrate the property of monotone convergence when mode B is considered for all blocks combined with centroid or factorial schemes. However, the absence of proof regarding the convergence of the error towards zero in Hanafi-Wold's procedure is a limitation compared to alternative procedure, which possesses this convergence property. Therefore, this paper aims to establish the convergence of the error towards zero in Hanafi-Wold's procedure.

Keywords Partial Least Squares Path Modelling, Hanafi-Wold's procedure, SLM procedure, Lohmöller's procedure

DOI: 10.19139/soic-2310-5070-2223

1. Introduction

Partial Least Squares Path Modeling (PLS-PM) is a statistical methodology extensively applied in structural equation modeling (SEM), with significant popularity in diverse fields such as business, marketing, and the social sciences [1, 10]. Its primary purpose is to evaluate relationships between latent (unobservable) variables using observed variables, commonly referred to as Manifest Variables (MVs), serving as indicators for measuring the latent variables. PLS-PM enables researchers to explore intricate relationships among multiple blocks of observed variables, each summarized by a weighted composite and assumed to measure a construct.

Originally developed by Herman Wold [16, 17] , PLS-PM stands as an alternative to covariance structure analysis [7] in Structural Equation Modeling, emphasizing distinct approaches and resulting in different parametrizations. Numerous research fields, including behavioral sciences and various disciplines within business research such as marketing, strategy, and management information systems, have embraced PLS-PM for its specific advantages [8]. It proves particularly valuable in handling complex models, non-normal data, and situations with small sample sizes, excelling in predictive modeling and managing both measurement and structural models simultaneously.

Herman O. A. Wold's positioning of PLS-PM as "soft modeling" reflects its adaptability to handle diverse and less-than-ideal data conditions compared to the more rigid assumptions associated with covariance-based structural equation modeling.

PLS-PM's flexibility, ability to handle non-normal data, focus on predictive performance, and ease of use make it a suitable choice for researchers dealing with small sample sizes. It provides a practical alternative when traditional SEM methods face challenges in such scenarios.

*Correspondence to: Abderrahim Sahli (Email: abderrahim.sahli@um5r.ac.ma). Mathematics, Statistics, and Applications Laboratory, Faculty of sciences, Mohammed V University in Rabat, Morocco.

ISSN 2310-5070 (online) ISSN 2311-004X (print)

Overall, the implementation of PLS-PM in various software with graphical interfaces, such as SmartPLS and PLS-Graph, XLSTAT-PLSPM [15, 18], has played a significant role in making PLS-PM more attractive and accessible to a broader audience. The ease of use and visualization features contribute to the broader adoption of PLS-PM in diverse fields of research.

In the formal framework of PLS-PM, the assumption is that the entirety of information concerning the relationships among K blocks of observable variables, referred to as $\mathbf{X}_1, \mathbf{X}_2, \ldots, \mathbf{X}_K$, is effectively captured by K components denoted as $\mathbf{z}_1, \mathbf{z}_2, \ldots, \mathbf{z}_K$. Each component $\mathbf{z}_k$ serves as an operationalization of the corresponding construct, denoted as $\boldsymbol{\xi}_k$, which is not directly observable. $\boldsymbol{\xi}_k$ is presumed to represent a block of p_k Manifest Variables (MVs), denoted as $\mathbf{X}_k = [\mathbf{x}_{k,1}, \mathbf{x}_{k,2}, \ldots, \mathbf{x}_{k,p_k}]$. These diverse blocks of MVs are measured across the same set of N observations and organized in matrices $\mathbf{X}_1, \mathbf{X}_2, \ldots, \mathbf{X}_K$.

In PLS-PM analysis, researchers develop a conceptual path model known as a path diagram (see figure 1). In this diagram, paths symbolize hypothesized causal relationships between a block of variables, and the magnitude of these relationships is quantified using parameters (path coefficients and Loadings). The Manifest Variables (MVs) $\mathbf{x}_{k,j}$ $(1 \leq k \leq K; 1 \leq j \leq p_k)$ are represented as squares, while constructs $\boldsymbol{\xi}_k$, $(1 \leq k \leq K)$ are depicted as circles in this visual representation.

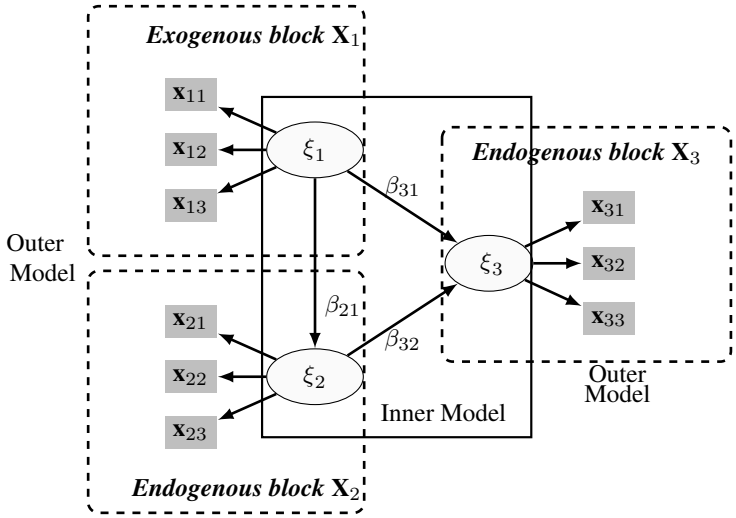

Figure 1. Conceptual Model involving 3 blocks of manifest variables.

PLS-PM involves two models : (i) the outer or measurement model and (ii) the inner or structural model. The outer model delineates relationships between a latent variable and its observed indicators or manifest variables through simple regression. Each path in the outer model corresponds to a specific loading, quantifying the strength of the relationship between a manifest variable and its corresponding latent variable. Formally, the relationship between each Manifest Variable (MV) $\mathbf{x}_{k,j}$ and its corresponding construct $\boldsymbol{\xi}_k$ is defined by the following equation $(1 \leq j \leq p_k; 1 \leq k \leq K)$:

$$\mathbf{x}_{k,j} = \pi^0_{k,j} + \pi_{k,j}\boldsymbol{\xi}_k + \boldsymbol{\epsilon}_{k,j}. \tag{1}$$

Although there are no necessary assumptions about the error distribution, it is presumed that the errors $(\boldsymbol{\epsilon}_{k,j})$ have a zero mean and are independent of the construct $\boldsymbol{\xi}_k$. This assumption is referred to as the predictor specification condition and entails the following :

$$E\left(\mathbf{x}_{k,j}|\boldsymbol{\xi}_k\right) = \pi^0_{k,j} + \pi_{k,j}\boldsymbol{\xi}_k \quad (1 \leq j \leq p_k, 1 \leq k \leq K) \tag{2}$$

The inner model specifies relationships between latent variables. In this model, a dependent construct $\boldsymbol{\xi}_{k'}$ is connected to the corresponding predictor constructs $\boldsymbol{\xi}_k$, with $k \in J_{k'}$, $\quad J_{k'} = \{k : \boldsymbol{\xi}_{k'}$ is predicted by $\boldsymbol{\xi}_k\}$, and its prediction is carried out using a simple or multiple regression, as follows

$$\boldsymbol{\xi}_{k'} = \beta_{k'}^0 + \sum_{k \in J_{k'}} \beta_{k'k} \boldsymbol{\xi}_k + \boldsymbol{\delta}_{k'} \tag{3}$$

The standard assumptions concerning the residuals, as suggested by the predictor specification condition, are put forth.

In the structural model, the relationships between latent variables are quantified by path coefficients. These relationships can also be represented in a binary manner using an adjacency matrix. This matrix, denoted by $\mathbf{C} = [c_{kl}]$ is a (K, K) binary square matrix where each element indicates whether a link exists between two constructs. Specifically, $c_{kl} = c_{lk} = 1$ if there is a connection between the constructs ξ_k and ξ_l, and $c_{kl} = c_{lk} = 0$ otherwise. Additionally, for each construct, $c_{kk} = 0$, (for $k = 1, 2, \cdots, K$).

The adjacency matrix $\mathbf{C}$ represents the relationships between latent variables, where each element indicates the presence or absence of a link between two variables. From this matrix, we define the Signless Laplacian matrix as $\mathbf{D} + \mathbf{C}$, where $\mathbf{D} = [d_{kl}]$ is a (*K*,*K*) diagonal matrix. Each diagonal element d_{kk} represents the degree of construct ξ_k, which is the number of edges incident to vertex ξ_k. Additionally, the k^{th} diagonal element d_{kk} of $\mathbf{D}$ is given by the sum of the elements in the k^{th} row of $\mathbf{C}$, i.e., $d_{kk} = \sum_{l=1}^{K} c_{kl}$.

The PLS-PM algorithm unfolds in three stages [16]. In the first stage, it iteratively calculates the outer weights $\mathbf{w}_k$, which are crucial for determining the components $\mathbf{z}_k = X_k \mathbf{w}_k \ (1 \leq k \leq K)$ as a linear combination of its MVs, the weights $\mathbf{w}_k$ are normalized to ensure the component has unit variance, $\dfrac{\mathbf{w}_k^\top \mathbf{X}_k^\top \mathbf{X}_k \mathbf{w}_k}{N} = 1$. The second stage involves estimating model parameters, including loadings and path coefficients (i.e. the parameters $\pi_{k,j}$ $(1 \leq j \leq p_k, 1 \leq k \leq K)$ and $\beta_{k'k}$ in equations (1) and (3)). The third stage entails the estimation of the location parameters $\pi_{k,j}^0$, $(1 \leq j \leq p_k, 1 \leq k \leq K)$ and $\beta_{k'}^0$.

Currently, there are three iterative procedures available for the computation of components $\mathbf{z}_k \ (1 \leq k \leq K)$ [5] : Hanafi-Wold's, Lohmöller's and SLM procedures, specifically addressing the initial stage of the PLS-PM algorithm. Each procedure offers six potential methods for computing the components : (i) two distinct methodologies for computing the outer weights for each block, designated as mode *A* or mode *B*. (ii) Three choices for all blocks, known as centroid, factorial, or path weighting schemes.

The error associated with these procedures, denoted by $\delta^{(s)}$, is the sum of the differences between the estimated scores of latent variables across two successive iterations, is given as

$$\delta^{(s)} = \frac{1}{K} \sum_{k=1}^{K} \left\| \mathbf{z}_k^{(s+1)} - \mathbf{z}_k^{(s)} \right\|^2 \tag{4}$$

where $\mathbf{z}_k^{(s)}$ and $\mathbf{z}_k^{(s+1)}$ represent the components calculated at iteration (s) and iteration $(s+1)$, respectively.

The quantity $\delta^{(s)}$, representing the overall change in the model between two successive iterations, this error used to evaluate the accuracy of the algorithms by observing the reduction of this error from one iteration to the next. The error $\delta^{(s)}$ is theoretically expected to converge to zero as iterations progress, indicating that the latent variable scores become stationary and the model reaches equilibrium. The convergence of this error is a key indicator of the model's stability and the accuracy of the estimated scores.

In the following, by the monotone convergence of a sequence of vectors $\mathbf{v}^{(s)}$, $s = 1, 2, \ldots$, we refer to the existence of a criterion f, a continuous bounded function, such that the real-valued sequence $f\left(\mathbf{v}^{(s)}\right), s = 1, 2, ...,$ obtained by applying f to $\mathbf{v}^{(s)}$, is monotone (i.e., either increasing or decreasing). This implies that the function f, when applied to the sequence $\mathbf{v}^{(s)}$, $s = 1, 2, \ldots$, ensures the monotonicity of the criterion $f\left(\mathbf{v}^{(s)}\right)$ over successive iterations, ultimately leading to convergence. By monotone convergence of a procedure, we mean that the sequence

of components generated by this procedure converges monotonically according to a certain criterion.

The absence of a formal proof of convergence for the PLS-PM algorithm has been a topic of interest and concern within the research community [3, 5, 6]. While PLS-PM is widely used in practice and has shown effectiveness in various applications, the lack of a rigorous mathematical proof of convergence has led researchers to seek and explore this proof. Researchers and practitioners should stay informed about developments in the field to understand the strengths and limitations of PLS-PM in various contexts [5].

Both SLM and Hanafi-Wold's procedures have been proven to converge monotonically. [3] demonstrates that Hanafi-Wold's procedure exhibits monotone convergence, while [5] establishes the same property for SLM. This means that the sequence of components generated by each procedure consistently increases a specific criterion, leading to convergence. In other words, both SLM and Hanafi-Wold's procedures aim to optimize the following criterion

$$\textbf{(MP)} \begin{cases} \underset{\mathbf{w}_1,\ldots,\mathbf{w}_k}{\text{maximize}} \quad \rho\left(\mathbf{w}_1,\ldots,\mathbf{w}_k\right) = \underset{\mathbf{w}_1,\ldots,\mathbf{w}_K}{\text{maximize}} \sum_{l,k=1}^{K} \left(c_{kl} + \tau d_{kl}\right) \phi\left(\mathbf{w}_k^\top \mathbf{X}_k^\top \mathbf{X}_l \mathbf{w}_l\right) \\ \text{s.t. } \mathbf{w}_k^\top \mathbf{X}_k^\top \mathbf{X}_k \mathbf{w}_k = 1, k = 1,\ldots,K \end{cases}$$

where $\tau = 0$ for the Hanafi-Wold procedure and $\tau = 1$ for the SLM procedure, and $\phi(x)$ si a real-valued function of the scalar $x \in \mathbb{R}$ such that

$$\phi(x) = \begin{cases} |x| & \text{centroid} \\ x^2 & \text{factorial} \end{cases} \tag{5}$$

The convergence of the error is another key concept when evaluating the performance of SLM and Hanafi-Wold's procedures. Specifically, it refers to whether the sequence $\left(\delta^{(s)}\right)_{s=0,1,\ldots}$, as defined in equation (4), converges to zero, ensuring that the gap between successive iterations progressively decreases. This error convergence is crucial for assessing the accuracy of the algorithms, ensuring that they not only converge monotonically but also demonstrate continuous improvement in solution quality. In other words, as the algorithm progresses, the error $\delta^{(s)}$ between successive iterations diminishes, leading to more precise convergence toward the optimal solution.

Table 1. Convergence issues and results when mode *B* is considered for all blocks.

Procedure	Scheme	Monotony convergence	Error convergence
Hanafi-Wold	Centroid	Yes	Unknown
	Factorial	[3]	Unknown
	Path	Unknown	Unknown
SLM	Centroid	Yes	Yes
	Factorial	[5]	[5]
	Path	Unknown	Unknown

When mode *B* is applied to all blocks, table 1 provides a summary of convergence issues and results for the SLM and Hanafi-Wold procedures. As demonstrated by [5], combining mode *B* with centroid or factorial schemes leads to the convergence of the sequence $\left(\delta^{(s)}\right)_{s=0,1,\ldots}$ toward zero in the SLM procedure. Recent research by [4] supports the convergence of the error in Hanafi-Wold's procedure. However, the findings presented in [4] are not sufficient to conclude that the sequence $\left(\delta^{(s)}\right)_{s=0,1,\ldots}$ converges to zero in all cases.
Motivated by this matter, we were inspired to delve into exploration and actively search for a mathematical proof of convergence of the error of Hanafi-Wold's procedure.

In the current paper, we will provide an exhaustive and rigorous proof illustrating the convergence of the error towards zero in the Hanafi-Wold procedure. This analysis will persist in mode B for all blocks combined with centroid or factorial schemes.

The present paper is organized as follows. In Section 2, we provide a brief overview of the SLM and Hanafi-Wold procedures. A compact form of Hanafi-Wold's procedure is presented in Section 3, along with a discussion of its theoretical outcomes concerning the previously established convergence properties of Hanafi-Wold's procedure. The establishment of error convergence for Hanafi-Wold's procedure is demonstrated in Section 4. Section 5 includes several simulations and comparisons involving Hanafi-Wold's procedure. Finally, Section 6 outlines the conclusions and future perspectives. Proofs for several lemmas are provided in Appendix A.

2. SLM and Hanafi-Wold's procedures

This section provides a synopsis of the SLM and Hanafi-Wold procedures, which involve the calculation of vectors of weights $\mathbf{w}_k\ (1 \leq k \leq K)$, used in computing $\mathbf{z}_k = \mathbf{X}_k\mathbf{w}_k; (1 \leq k \leq K)$. The components $\mathbf{z}_k$ are constrained to be centered and have unit variance $\left(\dfrac{\mathbf{w}_k^\top \mathbf{X}_k^\top \mathbf{X}_k \mathbf{w}_k}{N} = 1\right)$. Both procedures entail iteratively constructing K sequences of components $\mathbf{z}_k^{(s)} = \mathbf{X}_k\mathbf{w}_k^{(s)}\ (1 \leq k \leq K)$ and $(s = 0, 1, 2, \ldots)$, as described in Table 2.

Table 2. SLM and Hanafi-Wold's procedures

SLM procedure	Hanafi-Wold's procedure
1. $r_{kl}^{(s)} = \text{cor}(\mathbf{z}_k^{(s)}, \mathbf{z}_l^{(s)})$	1. $r_{kl}^{(s)} = \begin{cases} \text{cor}(\mathbf{z}_k^{(s)}, \mathbf{z}_l^{(s+1)}) & l < k \\ \text{cor}(\mathbf{z}_k^{(s)}, \mathbf{z}_l^{(s)}) & l > k \end{cases}$
2. $\theta_{kl}^{(s)} = \begin{cases} \text{sign}(r_{kl}^{(s)}) & \textit{Centroid} \\ r_{kl}^{(s)} & \textit{Factorial} \end{cases}$	2. $\theta_{kl}^{(s)} = \begin{cases} \text{sign}(r_{kl}^{(s)}) & \textit{Centroid} \\ r_{kl}^{(s)} & \textit{Factorial} \end{cases}$
3. $\mathbf{Z}_k^{(s)} = \sum_{l=1}^{K} c_{kl}\theta_{kl}^{(s)}\mathbf{z}_l^{(s)}$	3. $\mathbf{Z}_k^{(s)} = \sum_{l=1}^{k-1} c_{kl}\theta_{kl}^{(s)}\mathbf{z}_l^{(s+1)} + \sum_{l=k+1}^{K} c_{kl}\theta_{kl}^{(s)}\mathbf{z}_l^{(s)}$
4. $\tilde{\mathbf{w}}_k^{(s+1)} = \begin{cases} d_{kk}\mathbf{w}_k^{(s)} + \mathbf{X}_k^\top \mathbf{Z}_k^{(s)} & \textit{mode A} \\ d_{kk}\mathbf{w}_k^{(s)} + (\mathbf{X}_k^\top \mathbf{X}_k)^{-1}\mathbf{X}_k^\top \mathbf{Z}_k^{(s)} & \textit{mode B} \end{cases}$	4. $\tilde{\mathbf{w}}_k^{(s+1)} = \begin{cases} \mathbf{X}_k^\top \mathbf{Z}_k^{(s)} & \textit{mode A} \\ (\mathbf{X}_k^\top \mathbf{X}_k)^{-1}\mathbf{X}_k^\top \mathbf{Z}_k^{(s)} & \textit{mode B} \end{cases}$
5. $\mathbf{w}_k^{(s+1)} = \sqrt{n}\,\dfrac{\tilde{\mathbf{w}}_k^{(s+1)}}{\left\|\mathbf{X}_k\tilde{\mathbf{w}}_k^{(s+1)}\right\|}$	5. $\mathbf{w}_k^{(s+1)} = \sqrt{N}\,\dfrac{\tilde{\mathbf{w}}_k^{(s+1)}}{\left\|\mathbf{X}_k\tilde{\mathbf{w}}_k^{(s+1)}\right\|}$
6. $\mathbf{z}_k^{(s+1)} = \mathbf{X}_k\mathbf{w}_k^{(s+1)}$	6. $\mathbf{z}_k^{(s+1)} = \mathbf{X}_k\mathbf{w}_k^{(s+1)}$

The path weighting scheme is excluded from consideration in this paper. Each iteration begins with an arbitrary selection of components, and the sequences of components $\mathbf{z}_1^{(s)}, \mathbf{z}_2^{(s)}, \ldots, \mathbf{z}_K^{(s)}$ are generated following steps 1 to 6. The iteration continues over (s) until the quantity $\delta^{(s)}$ is less than or equal to a predefined threshold.

SLM and Hanafi-Wold's procedures compute the component based on the selected mode for determining outer weights (step 4). The decision between the two modes extends beyond the specified measurement model. In Mode A, a simple linear regression is applied to each Manifest Variable (MV) using the corresponding composite computed in the inner step (step 3). In contrast, Mode B utilizes multiple linear regression, with each composite (computed in step 3) regressed against the corresponding Manifest Variables (MVs).

As for the inner scheme (step 2), both procedures depend on two schemes (centroid or factorial), based on how $\theta_{kl}^{(s)}$ is calculated, factorial and centroid schemes typically yield very similar results. However, given that the factorial scheme considers the strength of the correlation, whereas the centroid scheme only takes the sign of the correlation into account, the factorial scheme is preferable when the correlation between components is close to zero. Throughout the iteration cycles, the correlation may oscillate from small negative to small positive values.

The main difference between the two procedures lies in the computation of $\mathbf{Z}_k^{(s)}$ (step 3). In SLM procedure, at iteration $(s+1)$, each component $\mathbf{z}_k^{(s+1)}$ $(1 \leq k \leq K)$ is computed as a function of all the components $\mathbf{z}_k^{(s)}$ $(1 \leq k \leq K)$ obtained during the previous step (s).

On the other hand, Hanafi-Wold's procedure operates differently. At iteration $(s+1)$, it calculates the component $\mathbf{z}_k^{(s+1)}$ associated with block $\mathbf{X}_k$ based on the components from the current iteration $(s+1)$: $\mathbf{z}_1^{(s+1)}, \mathbf{z}_2^{(s+1)}, \ldots, \mathbf{z}_{k-1}^{(s+1)}$, for the preceding blocks $\mathbf{X}_1, \mathbf{X}_2, \ldots, \mathbf{X}_{k-1}$, as well as the components from the previous iteration (s): $\mathbf{z}_{k+1}^{(s)}, \mathbf{z}_{k+2}^{(s)}, \ldots, \mathbf{z}_K^{(s)}$ for the blocks $\mathbf{X}_{k+1}, \mathbf{X}_{k+2}, \ldots, \mathbf{X}_K$. This allows it to adjust better and build on updated information at each step. In contrast, SLM procedure only uses the results from the previous iteration (s), making it less dynamic in its adjustments. As a result, it needs to perform more calculations at each iteration to reach the same solution, which slows down its convergence compared to Hanafi-Wold's procedure.

3. Compact form of Hanafi-Wold's procedure

The Hanafi-Wold's procedure can be presented in a compact form, depending on the two chosen schemes (i.e., centroid or factorial). For the centroid scheme, the procedure can be presented as follows :

$$\begin{cases} \Sigma_{l=1}^{k-1} c_{k,l} \operatorname{sign}\left(r\left(\mathbf{z}_k^{(s)}, \mathbf{z}_l^{(s+1)}\right)\right)\left(\mathbf{X}_k^\top \mathbf{X}_k\right)^{-1} \mathbf{X}_k^\top \mathbf{X}_l \mathbf{w}_l^{(s+1)} + \\ +\Sigma_{l=k+1}^{K} c_{k,l} \operatorname{sign}\left(r\left(\mathbf{z}_k^{(s)}, \mathbf{z}_l^{(s)}\right)\right)\left(\mathbf{X}_k^\top \mathbf{X}_k\right)^{-1} \mathbf{X}_k^\top \mathbf{X}_l \mathbf{w}_l^{(s)} = \lambda_k^{(s)} \mathbf{w}_k^{(s+1)} \\ \frac{\mathbf{w}_k'^{(s)} \mathbf{X}_k^\top \mathbf{X}_k \mathbf{w}_k^{(s)}}{N} = 1 \\ k = 1, 2, \ldots, K, \end{cases} \tag{6}$$

where

$$\begin{cases} \lambda_k^{(s)} = \frac{1}{\sqrt{N}} \left\| \mathbf{X}_k \left(\mathbf{X}_k^\top \mathbf{X}_k\right)^{-1} \mathbf{X}_k^\top \mathbf{Z}_k^{(s)} \right\|, \\ \mathbf{Z}_k^{(s)} = \Sigma_{l=1}^{k-1} c_{k,l} \operatorname{sign}\left(r_{kl}^{(s)}\right) \mathbf{z}_l^{(s+1)} + \Sigma_{l=k+1}^{K} c_{k,l} \operatorname{sign}\left(r_{kl}^{(s)}\right) \mathbf{z}_l^{(s)}. \end{cases} \tag{7}$$

For the factorial scheme, the procedure can be presented as follows :

$$\begin{cases} \Sigma_{l=1}^{k-1} c_{k,l} r\left(\mathbf{z}_k^{(s)}, \mathbf{z}_l^{(s+1)}\right)\left(\mathbf{X}_k^\top \mathbf{X}_k\right)^{-1} \mathbf{X}_k^\top \mathbf{X}_l \mathbf{w}_l^{(s+1)} + \\ +\Sigma_{l=k+1}^{K} c_{k,l} r\left(\mathbf{z}_k^{(s)}, \mathbf{z}_l^{(s)}\right)\left(\mathbf{X}_k^\top \mathbf{X}_k\right)^{-1} \mathbf{X}_k^\top \mathbf{X}_l \mathbf{w}_l^{(s)} = \mu_k^{(s)} \mathbf{w}_k^{(s+1)} \\ \frac{\mathbf{w}_k'^{(s)} \mathbf{X}_k^\top \mathbf{X}_k \mathbf{w}_k^{(s)}}{N} = 1 \\ k = 1, 2, \ldots, K, \end{cases} \tag{8}$$

where

$$\begin{cases} \mu_k^{(s)} = \frac{1}{\sqrt{N}} \left\| \mathbf{X}_k \left(\mathbf{X}_k^\top \mathbf{X}_k\right)^{-1} \mathbf{X}_k^\top \mathbf{Z}_k^{(s)} \right\|, \\ \mathbf{Z}_k^{(s)} = \Sigma_{l=1}^{k-1} c_{k,l} r_{kl}^{(s)} \mathbf{z}_l^{(s+1)} + \Sigma_{l=k+1}^{K} c_{k,l} r_{kl}^{(s)} \mathbf{z}_l^{(s)}. \end{cases} \tag{9}$$

The compact forms (6) and (8) are directly derived by substituting steps 3 and 4 into step 5 in Hanafi-Wold's procedure.

Subsequently, we delve into theoretical findings regarding the previously established convergence properties of Hanafi-Wold's procedure.

Theorem 1 presented below establishes the monotonic properties for Hanafi-Wold's procedure when using mode B in combination with centroid or factorial schemes.

Theorem 1 ([4]).
Let $\mathbf{z}_k^{(s)} = \mathbf{X}_k \mathbf{w}_k^{(s)} (1 \leq k \leq K)$, $s = 0, 1, 2, ...$, *be a sequence of LVs scores generated by Hanafi-Wold's*

procedure, when the centroid or factorial schemes are considered the following equality holds :

$$\rho\left(\mathbf{z}_1^{(s+1)},\mathbf{z}_2^{(s+1)},\cdots,\mathbf{z}_K^{(s+1)}\right)-\rho\left(\mathbf{z}_1^{(s)},\mathbf{z}_2^{(s)},\cdots,\mathbf{z}_K^{(s)}\right)=\frac{1}{N}\begin{cases}\sum_{k=1}^{K}\lambda_k^{(s)}\left\|\mathbf{z}_k^{(s+1)}-\mathbf{z}_k^{(s)}\right\|^2 & \textit{centroid}\\ \sum_{k=1}^{K}\mu_k^{(s)}\left\|\mathbf{z}_k^{(s+1)}-\mathbf{z}_k^{(s)}\right\|^2 & \textit{factorial}\end{cases} \tag{10}$$

where ρ is given as the following :

$$\rho\left(\mathbf{z}_1,\mathbf{z}_2,\cdots,\mathbf{z}_K\right)=\sum_{k,l=1,k\neq l}^{K}c_{kl}\phi\left(r\left(\mathbf{z}_k,\mathbf{z}_l\right)\right), \tag{11}$$

ϕ, $\lambda_k^{(s)}$ and $\mu_k^{(s)}$ are provided in equations (5), (7) and (9) respectively.

As a direct result of theorem 1 , the monotonic convergence of Hanafi-Wold's procedure has been established.

In the next section, we will rigorously demonstrate that the error in the Hanafi-Wold procedure converges to zero. This convergence is a key indicator of the procedure's stability and efficiency, ensuring consistent results with each iteration. This step is crucial for validating the method's relevance in the PLS-PM approach, reinforcing its position as one of the most effective algorithms.

4. Convergence of the error of Hanafi-Wold's procedure

When mode B is applied to all blocks combined with the centroid or factorial schemes, an equivalent form for Hanafi-Wold's procedure is introduced. The significance of this equivalent form lies in the highlighting of a matrix that plays an important role in this paper.

By setting $\mathbf{u}_k=\left(\frac{\mathbf{X}_k^\top\mathbf{X}_k}{N}\right)^{1/2}\mathbf{w}_k$, and $\mathbf{P}_k=\mathbf{X}_k\left(\frac{\mathbf{X}_k^\top\mathbf{X}_k}{N}\right)^{-1/2}$ in the optimization problem **(MP)**, this later becomes

$$\underset{\mathbf{u}\in\Omega}{\text{maximize}}\quad\rho(\mathbf{u})=\underset{\mathbf{u}_1,\ldots,\mathbf{u}_k}{\text{maximize}}\quad\rho\left(\mathbf{u}_1,\ldots,\mathbf{u}_k\right)=\sum_{l,k=1}^{K}c_{lk}\phi\left(\mathbf{u}_k^\top\mathbf{P}_k^\top\mathbf{P}_l\mathbf{u}_l\right) \tag{12}$$

subject to $\mathbf{u}_k\in\Omega_k$ for all $k=1,\ldots,K$ with $\Omega_k=\left\{\mathbf{u}_k\in\mathbb{R}^{p_k};\mathbf{u}_k^\top\mathbf{u}_k=1\right\}$, Ω equals the Cartesian product of the sets $\Omega_k\left(\Omega=\Omega_1\otimes\Omega_2\otimes\ldots\otimes\Omega_K\right)$, and $\mathbf{u}=\left(\mathbf{u}_1^\top,\mathbf{u}_2^\top,\ldots,\mathbf{u}_K^\top\right)^\top$.

Lemma 1 announces this equivalent form for Hanafi-Wold's procedure.

Lemma 1. *The sequence of components generated by Hanafi-Wold's procedure applied to $\mathbf{X}_k$ $(k=1,2\cdots,K)$ and initialized by $\mathbf{z}_k^{(0)}$ $(k=1,2\cdots,K)$ is identical to the sequence of components generated by the same procedure applied to $\mathbf{P}_k=\mathbf{X}_k\left(\frac{\mathbf{X}_k^\top\mathbf{X}_k}{N}\right)^{-1/2}$ $(k=1,2\cdots,K)$ and initialized by the same $\mathbf{z}_k^{(0)}$ $(k=1,2\cdots,K)$.*

The proof of lemma 1 can be found in appendix A.

Lemma 1 establishes the equivalence between two formulations of Hanafi-Wold's procedure, as outlined in table 3. Equivalent findings have been demonstrated for alternative procedures [5]. Additionally, it clarifies the connection between modes *A* and *B*. Mode *B* can be regarded as a special case of mode *A*. Specifically, Mode *B* applied to data $\mathbf{X}_k$ is identical to Mode *A* applied to $\mathbf{P}_k$ because $(\mathbf{P}_k{}^\top\mathbf{P}_k)^{-1}\mathbf{P}_k{}^\top=N\mathbf{P}_k{}^\top$ (see step 4 in table 3).

Before revealing the convergence result, it is crucial to establish several lemmas that play an important role in the following.

Table 3. Two equivalent forms of Hanafi-Wold's procedure with mode *B* for all blocks combined with the centroid or factorial schemes.

$\mathbf{X}_k \ \ (k=1,\ldots,K)$	$\mathbf{P}_k = \mathbf{X}_k \left(\frac{\mathbf{X'}_k\mathbf{X}_k}{N}\right)^{-1/2} \quad (k=1,\ldots,K)$
1. $r_{kl}^{(s)} = \begin{cases} cor(\mathbf{z}_k^{(s)}, \mathbf{z}_l^{(s+1)}) & l<k \\ cor(\mathbf{z}_k^{(s)}, \mathbf{z}_l^{(s)}) & l>k \end{cases}$	1. $r_{kl}^{(s)} = \begin{cases} cor(\mathbf{z}_k^{(s)}, \mathbf{z}_l^{(s+1)}) & l<k \\ cor(\mathbf{z}_k^{(s)}, \mathbf{z}_l^{(s)}) & l>k \end{cases}$
2. $\theta_{kl}^{(s)} = \begin{cases} sign\left(r_{kl}^{(s)}\right) & \textit{Centroid} \\ r_{kl}^{(s)} & \textit{Factorial} \end{cases}$	2. $\theta_{kl}^{(s)} = \begin{cases} sign\left(r_{kl}^{(s)}\right) & \textit{Centroid} \\ r_{kl}^{(s)} & \textit{Factorial} \end{cases}$
3. $\mathbf{Z}_k^{(s)} = \sum_{l=1}^{k-1} c_{kl}\theta_{kl}^{(s)}\mathbf{z}_l^{(s+1)} + \sum_{l=k+1}^{K} c_{kl}\theta_{kl}^{(s)}\mathbf{z}_l^{(s)}$	3. $\mathbf{Z}_k^{(s)} = \sum_{l=1}^{k-1} c_{kl}\theta_{kl}^{(s)}\mathbf{z}_l^{(s+1)} + \sum_{l=k+1}^{K} c_{kl}\theta_{kl}^{(s)}\mathbf{z}_l^{(s)}$
4. $\tilde{\mathbf{w}}_k^{(s+1)} = \begin{cases} {\mathbf{X}_k}^\top \mathbf{Z}_k^{(s)} & \textit{mode A} \\ ({\mathbf{X}_k}^\top \mathbf{X}_k)^{-1}{\mathbf{X}_k}^\top \mathbf{Z}_k^{(s)} & \textit{mode B} \end{cases}$	4. $\tilde{\mathbf{u}}_k^{(s+1)} = \begin{cases} {\mathbf{P}_k}^\top \mathbf{Z}_k^{(s)} & \textit{mode A} \\ {\mathbf{P}_k}^\top \mathbf{Z}_k^{(s)} & \textit{mode B} \end{cases}$
5. $\mathbf{w}_k^{(s+1)} = \sqrt{N}\frac{\tilde{\mathbf{w}}_k^{(s+1)}}{\left\|\mathbf{X}_k\tilde{\mathbf{w}}_k^{(s+1)}\right\|}$	5. $\mathbf{u}_k^{(s+1)} = \sqrt{N}\frac{\tilde{\mathbf{u}}_k^{(s+1)}}{\left\|\mathbf{P}_k\tilde{\mathbf{u}}_k^{(s+1)}\right\|}$
6. $\mathbf{z}_k^{(s+1)} = \mathbf{X}_k\mathbf{w}_k^{(s+1)}$	6. $\mathbf{z}_k^{(s+1)} = \mathbf{P}_k\mathbf{u}_\mathbf{k}^{(\mathbf{s+1})}$

Lemma 2. *For any vector* $\left(\mathbf{u}_1^\top, \ldots, \mathbf{u}_K^\top\right)^\top \in \Omega$ *and for all* $k = 1, 2, \cdots, K$, *we define the function* φ_k *as*

$$\varphi_k(\boldsymbol{v}_k) = \sum_{l=1, l\neq k}^{K} c_{kl}\theta_{kl}\boldsymbol{v}_k^\top \mathbf{P}_k^\top \mathbf{P}_l\mathbf{u}_l \tag{13}$$

such that $\theta_{kl} = \begin{cases} sign\left(cor\left(\mathbf{P}_k\mathbf{u}_k; \mathbf{P}_l\mathbf{u}_l\right)\right) & \textit{Centroid} \\ cor\left(\mathbf{P}_k\mathbf{u}_k; \mathbf{P}_l\mathbf{u}_l\right) & \textit{Factorial} \end{cases}$

Then the maximum of φ_k *on* Ω_k *is achieved for*

$$\bar{\mathbf{v}}_k = \frac{\sum_{l=1, l\neq k}^{K} c_{kl}\theta_{kl}\mathbf{P}_k^\top \mathbf{P}_l\mathbf{u}_l}{\left\|\sum_{l=1, l\neq k}^{K} c_{kl}\theta_{kl}\mathbf{P}_k^\top \mathbf{P}_l\mathbf{u}_l\right\|} \tag{14}$$

The proof of lemma 2 can be found in appendix A.

Lemma 3. *For any vector* $\left(\mathbf{u}_1^\top, \ldots, \mathbf{u}_K^\top\right)^\top \in \Omega$, *the following equalities hold :*

$$\rho\left(\bar{\mathbf{v}}_1, \bar{\mathbf{v}}_2, \cdots, \bar{\mathbf{v}}_K\right) - \rho\left(\mathbf{u}_1, \mathbf{u}_2, \cdots, \mathbf{u}_K\right) = 2\left(\sum_{k=1}^{K}\left(\varphi_k\left(\bar{\mathbf{v}}_k\right) - \varphi_k\left(\mathbf{u}_k\right)\right)\right) = \sum_{k=1}^{K}\alpha_k \left\|\mathbf{P}_k\bar{\mathbf{v}}_k - \mathbf{P}_k\mathbf{u}_k\right\|^2 \tag{15}$$

with $\alpha_k = \| \sum_{l=1, l\neq k}^{K} c_{kl}\theta_{kl}\mathbf{P}_k^\top \mathbf{P}_l\mathbf{u}_l \|$ *and* $\bar{\mathbf{v}}_k, k = 1, \ldots, K$ *given in (14)*

The proof of lemma 2 is available in Appendix A.
Theorem 2 below establishes the convergence of the error associated with Hanafi-Wold's procedure in computing components for the PLS-PM algorithm.

Theorem 2. *Let* $\mathbf{u}_k^{(s)}$ *be a sequence of weights generated by Hanafi-Wold's procedure, then the sequence* $\left(\mathbf{u}_k^{(s+1)} - \mathbf{u}_k^{(s)}\right)_{s=0,1,\ldots}$ *converges to 0, when the centroid or factorial schemes are considered.*

Proof
Let $\Phi_k : \Omega \to \Omega_k$ be a function defined as

$$\Phi_k\left(\mathbf{u}_1, \ldots, \mathbf{u}_K\right) = \frac{\sum_{l=1, l\neq k}^{K} c_{kl}\theta_{kl}\mathbf{P}_k^\top \mathbf{P}_l \mathbf{u}_l}{\left\| \sum_{l=1, l\neq k}^{K} c_{kl}\theta_{kl}\mathbf{P}_k^\top \mathbf{P}_l \mathbf{u}_l \right\|},$$

and $h_k : \Omega \to \Omega$ the function defined as $h_k\left(\mathbf{u}_1, \ldots, \mathbf{u}_K\right) = \left(\mathbf{u}_1, \ldots, \mathbf{u}_{k-1}, \Phi_k(\mathbf{u}), \mathbf{u}_{k+1}, \ldots, \mathbf{u}_K\right)$ and $h : \Omega \to \Omega$ the recurrence equation defined as $h = h_K \circ \ldots \circ h_1$. By construction, we have

$$\mathbf{u}^{(s+1)} = h\left(\mathbf{u}^{(s)}\right).$$

1. Suppose there are two subsequences $\left\{\mathbf{u}^{(n_s)}\right\}_{s=0}^{\infty}$ et $\left\{\mathbf{u}^{(n_s+1)}\right\}_{s=0}^{\infty}$ of $\left\{\mathbf{u}^{(s)}\right\}_{s=0}^{\infty}$, such that $\mathbf{u}^{(n_s)} \underset{n_s\to\infty}{\longrightarrow} \mathbf{u}$ and $\mathbf{u}^{(n_s+1)} \underset{n_s\to\infty}{\longrightarrow} \bar{\mathbf{v}}$, $\bar{\mathbf{v}} \neq \mathbf{u}$.
   By continuity of ρ we have $\rho(\mathbf{u}^{(n_s)}) \underset{n_s\to\infty}{\longrightarrow} \rho(\mathbf{u})$ and $\rho(\mathbf{u}^{(n_s+1)}) \underset{n_s\to\infty}{\longrightarrow} \rho(\bar{\mathbf{v}})$.

   (i) From the monotonic convergence of $\left\{\rho\left(\mathbf{u}^{(s)}\right)\right\}_{s=0}^{\infty}$ we get $\rho(\bar{\mathbf{v}}) = \rho(\mathbf{u})$.

   (ii) From continuity of h, it result that $\bar{\mathbf{v}} = h(\mathbf{u})$.

2. As $\bar{\mathbf{v}} \neq \mathbf{u}$ and $\bar{\mathbf{v}} = h(\mathbf{u})$, thus, there exist $k_0 \in \{1, \ldots, K\}$; $\bar{\mathbf{v}}_{k_0} \neq \mathbf{u}_{k_0}$.
   Since $\bar{\mathbf{v}}_{k_0}$ is the unique maximum of φ_{k_0} on Ω_{k_0}, then $\varphi_{k_0}(\bar{\mathbf{v}}_{k_0}) > \varphi_{k_0}(\mathbf{u}_{k_0})$ As

$$\rho(\bar{\mathbf{v}}) - \rho(\mathbf{u}) = \rho\big(\bar{\mathbf{v}}_1, \bar{\mathbf{v}}_2, \cdots, \bar{\mathbf{v}}_K\big) - \rho\big(\mathbf{u}_1, \mathbf{u}_2, \cdots, \mathbf{u}_K\big) = 2\left(\sum_{k=1}^{K}\big(\varphi_k\big(\bar{\mathbf{v}}_k\big) - \varphi_k\big(\mathbf{u}_k\big)\right) > 0$$

   This is a contradiction.

□

As a direct consequence of theorem 2 , the convergence of the error towards zero in Hanafi-Wold's procedure has been established.
As for each $k \in \{1, \ldots, K\}$ $\left\|\mathbf{z}_k^{(s+1)} - \mathbf{z}_k^{(s)}\right\| \leq \|\mathbf{P}_k\| \left\|\mathbf{u}_\mathbf{k}^{(\mathbf{s+1})} - \mathbf{u}_\mathbf{k}^{(\mathbf{s})}\right\|$,
then $\delta^{(s)} \leq \sum_{k=1}^{K} \frac{1}{K}\|\mathbf{P}_k\|^2 \left\|\mathbf{u}_\mathbf{k}^{(\mathbf{s+1})} - \mathbf{u}_\mathbf{k}^{(\mathbf{s})}\right\|^2$, using theorem 2, $\delta^{(s)}$ converges to 0.

The convergence of the sequence $\delta^{(s)}$ to 0 involves the sequence defined by the difference between two successive components $\left(\mathbf{z}_k^{(s+1)} - \mathbf{z}_k^{(s)}\right)_{s=0,1,\ldots}$ converging to 0 for each $k \in \{1, \ldots, K\}$. This implies that the latent variable scores become stationary and the model reaches equilibrium. The convergence of this error is a key indicator of the model's stability and the accuracy of the estimated scores.

5. Illustration and Numerical Comparisons

5.1. Illustration

After establishing a solid theoretical foundation with rigorous demonstrations, we now turn to the illustration of these results. This subsection will highlight the practical application of the conclusions using a relevant example or a well-known model in the literature. The objective is to validate the developed theories and demonstrate their relevance in real-world contexts.

The European Customer Satisfaction Index (ECSI) is a well-established model for measuring customer satisfaction across Europe. The ECSI model introduces seven interrelated latent variables (LVs) that provide a comprehensive framework for assessing factors such as image, customer expectations, perceived value, perceived quality, customer satisfaction, complaints, and customer loyalty. Widely applied in sectors like marketing and financial services, the model is grounded in well-established theories of customer behavior, making it applicable across various industries.

The study conducted by [14] applied the ECSI model to mobile phone consumers, highlighting the importance of measuring user satisfaction in this sector by considering factors such as image, customer expectations, perceived value, and perceived quality. A questionnaire was administered to a sample of 250 mobile phone consumers, resulting in a dataset called 'mobile' (see [14] for more details). This data set is available in the **semPLS** package [9].

We will apply SLM and Hanafi-Wold's procedures in the analysis of the mobile dataset extracted by [14], allowing us to evaluate the latent variable scores and validate the model's convergence properties. The algorithm iteratively computes the latent variable scores, refining the estimations at each step to ensure more accurate results

By following the classic structure of the ECSI model, we will evaluate the key latent variables that define customer satisfaction in this sector, including image, customer expectations, perceived value, and perceived quality. This model will provide actionable insights for enhancing the user experience and improving the competitiveness of mobile phone providers. Before computing the components, the dataset has been centered and standardized by columns. The adjacency matrix $\mathbf{C}$ and the signless laplacian matrix $\mathbf{D}+\mathbf{C}$, associated with this model, are given as follows

$$\mathbf{C}=\begin{pmatrix}0&1&0&0&1&0&1\\1&0&1&1&1&0&0\\0&1&0&1&1&0&0\\0&1&1&0&1&0&0\\1&1&1&1&0&1&1\\0&0&0&0&1&0&1\\1&0&0&0&1&1&0\end{pmatrix},\qquad \mathbf{D}+\mathbf{C}=\begin{pmatrix}3&1&0&0&1&0&1\\1&4&1&1&1&0&0\\0&1&3&1&1&0&0\\0&1&1&3&1&0&0\\1&1&1&1&6&1&1\\0&0&0&0&1&2&1\\1&0&0&0&1&1&3\end{pmatrix}.$$

Figures 2 and 3 present the results obtained from applying the SLM and Hanafi-Wold procedures to the mobile dataset. These figures highlight the differences and similarities between the two algorithms, emphasizing the key features of the results for each.

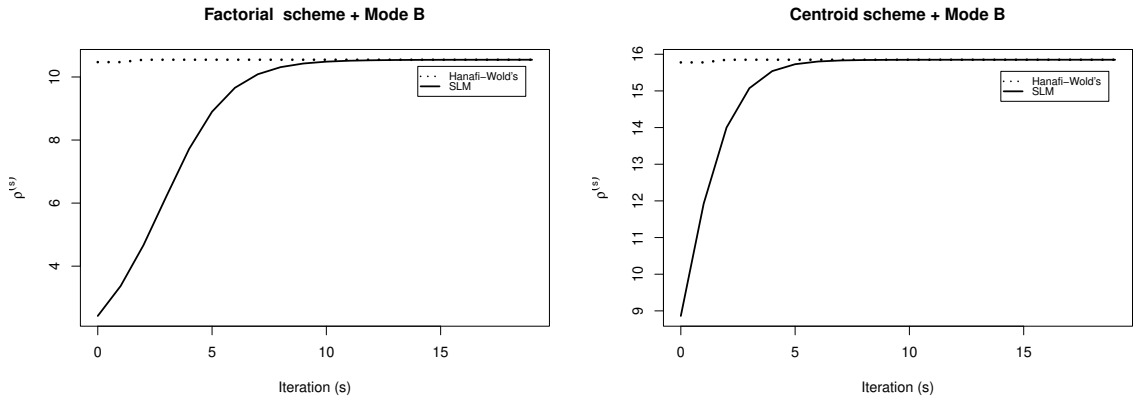

Figure 2. Left: Evolution of the criterion $\rho^{(s)}$ as a function of the number of iterations for the SLM and Hanafi-Wold procedures using mode *B* combined with the factorial scheme. Right: Evolution of the criterion $\rho^{(s)}$ as a function of the number of iterations for the SLM and Hanafi-Wold procedures using mode *B* combined with the centroid scheme.

Figure 2 illustrates the evolution of the criterion $\rho^{(s)}$ over the number of iterations for both the SLM and Hanafi-Wold procedures, using mode *B* combined with either the centroid or factorial schemes. The process stops once the fixed threshold of 10^{-7} is reached. Both procedures, SLM and Hanafi-Wold's, lead to an increase in the criterion , as shown in the figure.

The monotone convergence of the criteria $\rho^{(s)}$, as shown in figure 2 , is one such result, rigorously proven in theorem 1. Moreover, $\rho^{(s)}$ is a key criterion, reflecting the correlation between the estimated latent variables. As the algorithm progresses, these correlations increase, indicating that the estimated scores are becoming more consistent and aligned with each iteration. This improvement in correlation serves as an additional indicator of the model's accuracy and convergence, enhancing the robustness of the results.

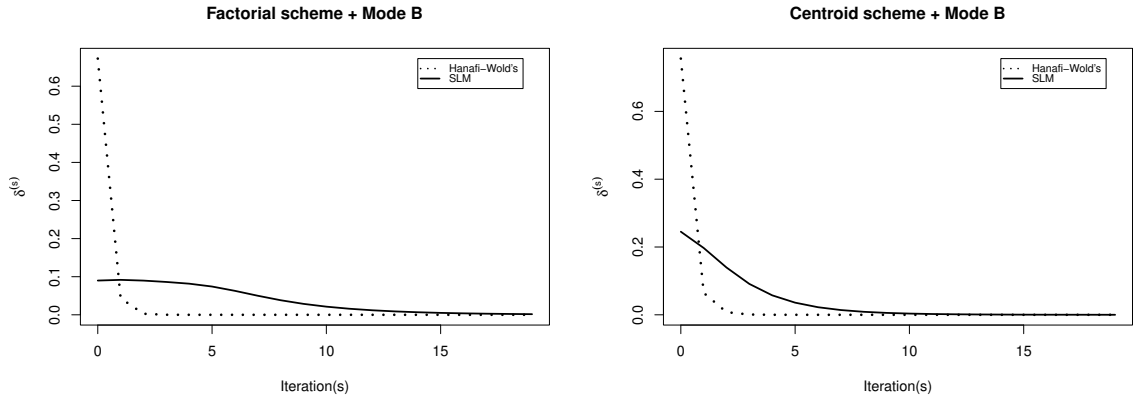

Figure 3. Left: Evolution of the error $\delta^{(s)}$ as a function of the number of iterations for the SLM and Hanafi-Wold procedures using mode *B* combined with the factorial scheme. Right: Evolution of the error $\delta^{(s)}$ as a function of the number of iterations for the SLM and Hanafi-Wold procedures using mode *B* combined with the centroid scheme.

Figure 3 shows the evolution of the error $\delta^{(s)}$ as a function of the number of iterations for the SLM and Hanafi-Wold procedures, using mode *B* combined with the centroid or factorial schemes, with the convergence tolerance set at the same fixed threshold.

Figure 3 illustrates that both SLM and Hanafi-Wold's procedures reduce the error over time, eventually converging to zero. Notably, Hanafi-Wold's procedure converges faster, requiring only 3 iterations compared to the 10 iterations of SLM in the centroid scheme. Similarly, for the factorial scheme, Hanafi-Wold's procedure achieves convergence in just 3 iterations, while SLM takes 15 iterations. This faster convergence indicates that Hanafi-Wold's procedure is more efficient in achieving the desired accuracy.

Furthermore, as the complexity of models increases with more latent variables, the difference in the number of iterations between the two algorithms becomes even more significant. This highlights the importance of choosing a more efficient algorithm for large-scale models, minimizing computation time and enhancing overall performance.

Moreover to converging more quickly, Hanafi-Wold's procedure also reduces its calculation error more effectively than SLM procedure. The differences between successive values decrease more rapidly, indicating better precision in the adjustments made at each iteration.

The superior performance of Hanafi-Wold's procedure is explained by its effective use of the most recent results from iteration $(s+1)$, as well as calculations from iteration (s). By exploring optimized directions, it adjusts more effectively and builds on updated information at each step.

In contrast, SLM procedure only uses the results from the previous iteration (s), making it less dynamic in its adjustments. As a result, it needs to perform more calculations at each iteration to reach the same solution, which slows down its convergence compared to Hanafi-Wold's procedure.

Additionally to converging faster and providing identical solutions to the SLM procedure. Hanafi-Wold's procedure also demonstrates greater stability across various simulation scenarios. This reinforces its reliability,

even when the initial conditions change. Therefore, along with its speed, Hanafi-Wold's procedure proves to be a robust and adaptable solution.

The convergence of the error $\delta^{(s)}$ towards 0, as shown in figure 3 , is one such result, which is rigorously proven in theorem 2. The outcomes in figure 3 reveal that the difference between the latent variable scores calculated in two successive iterations converges towards zero as the iterations progress. This indicates that both algorithms converge to the same solutions with increasing precision. This phenomenon of errors converging to zero demonstrates not only the stability of each algorithm but also their ability to refine the scores as the calculations proceed. In other words, the gradual reduction of the difference between successive scores is a strong sign that the algorithms are achieving increasingly precise and reliable results.

Furthermore, as we have theoretically shown, the differences between the scores across iterations converge to zero, meaning that the scores become stationary after a certain point. This convergence ensures that the model reaches an equilibrium where the estimated scores are sufficiently accurate and reliable. This process of monotone convergence and error reduction between successive iterations demonstrates the stability of the model and the continuous improvement of the estimated latent variable scores.

5.2. Comparison between SLM and Hanafi-Wold's procedures

Following the establishment of the theoretical foundations in Section 4, this subsection focuses on the comparison between the Hanafi-Wold and SLM procedures. The main objective is to assess their respective performance, particularly in terms of convergence speed, while also considering other relevant factors such as robustness and result stability. Although both algorithms exhibit similar convergence properties for mode B associated with the centroid and factorial schemes, it is essential to compare their performance not only in terms of iterations but also total computation time.

We will therefore highlight the general characteristics of these two approaches, aiming to shed light on their strengths and weaknesses in a practical context. Such a comparison will help determine which algorithm is best suited for specific needs, such as efficiency in speed or the complexity of the model or nature of the data being analyzed. This criterion allows for quantifying the efficiency of each algorithm and can be decisive in making one procedure the preferred solution over the other. Additionally, the comparison will also take into account the implementation conditions in large-scale environments, where performance differences could have significant consequences.

seven datasets from the literature, as shown in table 4, were used to conduct this analysis. For each dataset, the corresponding adjacency matrix was provided either in the referenced software or in the original source. Prior to calculating the components, each block from each dataset was centered and standardized by columns. For each dataset and for each combination of mode B with the centroid and factorial schemes, 100 randomly generated initializations were considered. Both procedures were initialized with the same starting point across all 100 attempts. The number of iterations required by each procedure to converge, using a threshold of 10^{-5} , was recorded.

Table 4. Names, characteristics and availability of 7 datasets

Data set	n	*K*	availability (package)
chickenk	351	5	ade4 [2]
rusett	47	3	RGCCA [13]
satisfaction	250	6	plspm [11]
simdata	400	3	plspm [11]
hanafi2007	10	3	semPLS [**?**]
simulated	200	4	multiblock [12]
mobi	250	7	semPLS [**?**]

Let κ represent the ratio defined as the average number of iterations required by Hanafi-Wold's procedure divided by the average number of iterations required by the SLM procedure. This ratio provides a simple yet effective measure for comparing the efficiency of the two algorithms in terms of convergence speed. If $\kappa \leq 1$, the iteration

gain is in favor of Hanafi-Wold's procedure, and the relative improvement is expressed as a percentage using the formula $100(1-\kappa)\%$. In this case, a lower κ indicates that Hanafi-Wold's procedure requires fewer iterations to reach convergence compared to SLM, thus demonstrating superior efficiency.

Conversely, if $\kappa > 1$, the iteration gain favors the SLM procedure. The gain in this scenario is calculated as $100(1-\kappa^{-1})\%$, highlighting how much more efficient SLM is compared to Hanafi-Wold's procedure. This difference in iteration count offers insight into which algorithm may be preferable for certain datasets or computational contexts, particularly when minimizing the number of iterations is critical for performance.

The results of the iteration and time gains between the two procedures, summarized respectively in tables 5 and 6, provide a detailed comparison and highlight the specific conditions under which each algorithm performs best. Analyzing these gains allows for an evaluation of the relative strengths of both methods, enabling a well-informed decision on the most suitable approach for practical applications.

Table 5. Gains on iterations of Hanafi World's procedure compared to SLM procedure

Dataset	Mode B	
Name	factorial (%)	centroid (%)
chickenk	95	87
rusett	83	78
satisfaction	82	77
simdata	87	80
hanafi2007	84	75
simulated	77	75
mobi	81	76

Table 6. Gains on time of Hanafi-Wold's procedure compared to the SLM procedure

Dataset	Mode B	
Name	factorial (%)	centroid (%)
chickenk	94	85
rusett	82	79
satisfaction	76	71
simdata	86	74
hanafi2007	82	74
simulated	74	73
mobi	76	68

As summarized in tables 5 and 6, the Hanafi-Wold procedure is generally faster than the SLM procedure. This is due to the fact that, at each iteration, the Hanafi-Wold procedure performs K optimizations to enhance the criterion ρ [3], whereas the SLM procedure only performs one. Consequently, in practical terms, the Hanafi-Wold procedure produces results more quickly, making it a more efficient option when computation time is a critical factor. This performance difference highlights the robustness of the Hanafi-Wold's algorithm, particularly in situations where numerous iterations would be required with the SLM procedure.

6. Conclusion and perspective

The paper addresses a critical issue in Partial Least Squares Path Modeling: the convergence of the error in the Hanafi-Wold procedure. We have provided a rigorous mathematical proof demonstrating that the error in Hanafi-Wold's procedure converges to zero when mode B is used in combination with centroid or factorial schemes.

Currently, the proof of error convergence is limited to mode B for all blocks combined with centroid or factorial schemes. While extending this proof to mode A, combined with the three schemes (centroid, factorial, and path

withing scheme), as well as for mode B with the path withing scheme, would be beneficial, this presents additional challenges. The complexity arises from the fact that monotonicity results for these alternative configurations, particularly for mode A and certain weighting schemes, have not yet been established.

It is important to note that the restriction of our proof to these specific configurations stems from the current lack of monotonicity results for other modes and schemes. The error convergence proof we present relies on monotonic convergence properties, which, in the context of the procedures we analyzed, have only been demonstrated for mode B in combination with the centroid and factorial schemes. Therefore, establishing convergence within these configurations already marks a significant advancement.

The decision to highlight these specific options is directly tied to the availability of robust monotonic convergence results for mode B. These results have allowed us to prove error convergence within this specific framework. However, similar results are not yet available for other modes or configurations. Extending the proof to these additional cases would thus require further advancements in understanding the monotonic convergence properties of these alternative configurations.

This opens up important avenues for future research. Exploring the possibility of monotonic convergence for modes like mode A, as well as for other weighting schemes, represents a promising direction for deepening the understanding of convergence properties in PLS-PM models. These future studies will help reinforce and generalize the current results to more varied configurations, expanding the practical applications of these methods.

Appendix A

Proof of lemma 1.

The proof is carried out through recurrence on the iteration s, where ${\mathbf{z}_k}^{(s)}$ represents the sequence of components generated by Hanafi-Wold's procedure applied to $(\mathbf{X}_1, ..., \mathbf{X}_K)$, initialized by the weights $\left(\tilde{\mathbf{w}}_1^{(0)}, ..., \tilde{\mathbf{w}}_K^{(0)}\right)$. ${\mathbf{y}_k}^{(s)}$ represents the sequence of components generated by Hanafi-Wold's procedure applied to $(\mathbf{P}_1, ..., \mathbf{P}_K)$, initialized by the weights $\left(\tilde{\mathbf{u}}_1^{(0)}, ..., \tilde{\mathbf{u}}_K^{(0)}\right)$ such that ${\mathbf{z}_k}^{(0)} = {\mathbf{y}_k}^{(0)}$ for each $k = 1, 2, \cdots, K$.

Suppose ${\mathbf{z}_k}^{(s)} = {\mathbf{y}_k}^{(s)}$ for all $s = 0, 1, 2, \ldots, s_0$. We have ${\mathbf{z}_1}^{(s_0+1)} = {\mathbf{y}_1}^{(s_0+1)}$. Suppose ${\mathbf{z}_l}^{(s_0+1)} = {\mathbf{y}_l}^{(s_0+1)}$ for all $l < k$. Let us show that ${\mathbf{z}_k}^{(s_0+1)} = {\mathbf{y}_k}^{(s_0+1)}$. For each block k at iteration $s_0 + 1$ we have :

$$
\begin{aligned}
\mathbf{z}_k^{(s_0+1)} = \mathbf{X}_k \mathbf{w}_k^{(s_0+1)} &= \sqrt{N} \frac{\mathbf{X}_k \tilde{\mathbf{w}}_k^{(s_0+1)}}{\left\| \mathbf{X}_k \tilde{\mathbf{w}}_k^{(s_0+1)} \right\|} \\
&= \sqrt{N} \frac{\mathbf{X}_k (\mathbf{X}_k{}^\top \mathbf{X}_k)^{-1} \mathbf{X}_k{}^\top {\mathbf{Z}_k}^{(s_0)}}{\left\| \mathbf{X}_k (\mathbf{X}_k{}^\top \mathbf{X}_k)^{-1} \mathbf{X}_k{}^\top {\mathbf{Z}_k}^{(s_0)} \right\|} \\
&= \sqrt{N} \frac{\mathbf{X}_k \left(\frac{\mathbf{X}_k{}^\top \mathbf{X}_k}{N} \right)^{-1} \mathbf{X}_k{}^\top \left(\sum_{l=1}^{k-1} c_{kl} \theta_{kl}^{(s_0)} \mathbf{z}_l^{(s_0+1)} + \sum_{l=k+1}^{K} c_{kl} \theta_{kl}^{(s_0)} \mathbf{z}_l^{(s_0)} \right)}{\left\| \mathbf{X}_k \left(\frac{\mathbf{X}_k{}^\top \mathbf{X}_k}{N} \right)^{-1} \mathbf{X}_k{}^\top \left(\sum_{l=1}^{k-1} c_{kl} \theta_{kl}^{(s_0)} \mathbf{z}_l^{(s_0+1)} + \sum_{l=k+1}^{K} c_{kl} \theta_{kl}^{(s_0)} \mathbf{z}_l^{(s_0)} \right) \right\|} \\
&= \sqrt{N} \frac{\mathbf{X}_k \left(\frac{\mathbf{X}_k{}^\top \mathbf{X}_k}{N} \right)^{-1/2} \left(\frac{\mathbf{X}_k{}^\top \mathbf{X}_k}{N} \right)^{-1/2} \mathbf{X}_k{}^\top \left(\sum_{l=1}^{k-1} c_{kl} \theta_{kl}^{(s_0)} \mathbf{z}_l^{(s_0+1)} + \sum_{l=k+1}^{K} c_{kl} \theta_{kl}^{(s_0)} \mathbf{z}_l^{(s_0)} \right)}{\left\| \mathbf{X}_k \left(\frac{\mathbf{X}_k{}^\top \mathbf{X}_k}{N} \right)^{-1/2} \left(\frac{\mathbf{X}_k{}^\top \mathbf{X}_k}{N} \right)^{-1/2} \mathbf{X}_k{}^\top \left(\sum_{l=1}^{k-1} c_{kl} \theta_{kl}^{(s_0)} \mathbf{z}_l^{(s_0+1)} + \sum_{l=k+1}^{K} c_{kl} \theta_{kl}^{(s_0)} \mathbf{z}_l^{(s_0)} \right) \right\|}
\end{aligned}
$$

Substituting $\mathbf{P}_k = \mathbf{X}_k \left(\frac{{\mathbf{X}_k}^\top \mathbf{X}_k}{N} \right)^{-1/2}$, it follows

$$\begin{aligned}
\mathbf{z}_k^{(s_0+1)} &= \sqrt{N} \frac{\mathbf{P}_k \mathbf{P}_k^\top \left(\sum_{l=1}^{k-1} c_{kl} \theta_{kl}^{(s_0)} \mathbf{z}_l^{(s_0+1)} + \sum_{l=k+1}^{K} c_{kl} \theta_{kl}^{(s_0)} \mathbf{z}_l^{(s_0)} \right)}{\left\| \mathbf{P}_k \mathbf{P}_k^\top \left(\sum_{l \neq k, l=1}^{K} c_{kl} \theta_{kl}^{(s_0)} \mathbf{z}_l^{(s_0)} \right) \right\|} \\
&= \sqrt{N} \frac{\mathbf{P}_k \left(\mathbf{P}_k^\top \mathbf{P}_k \right)^{-1} \mathbf{P}_k^\top \left(\sum_{l=1}^{k-1} c_{kl} \theta_{kl}^{(s_0)} \mathbf{z}_l^{(s_0+1)} + \sum_{l=k+1}^{K} c_{kl} \theta_{kl}^{(s_0)} \mathbf{z}_l^{(s_0)} \right)}{\left\| \mathbf{P}_k \left(\mathbf{P}_k^\top \mathbf{P}_k \right)^{-1} \mathbf{P}_k^\top \left(\sum_{l=1}^{k-1} c_{kl} \theta_{kl}^{(s_0)} \mathbf{z}_l^{(s_0+1)} + \sum_{l=k+1}^{K} c_{kl} \theta_{kl}^{(s_0)} \mathbf{z}_l^{(s_0)} \right) \right\|} \\
&= \mathbf{P}_k u_k^{(s_0+1)} \\
&= \mathbf{y}_k^{(s_0+1)}.
\end{aligned}$$

□

Proof of lemma 2.

For any $x, y \in \mathbb{R}^{p_k}$, $(1 \leq k \leq K)$, we have $\max_{x \in \mathbb{R}^{p_k}, \|x\|=1} x^\top y = \|y\|$.
The Cauchy-Schwarz inequality implies that $x^\top y \leq \|x\| \|y\| \leq \|y\|$. To demonstrate that the value is attained (i.e., it is equal to its upper bound), we observe that if $x = y/\|y\|$, then $x^\top y = \frac{y^\top y}{\|y\|} = \|y\|$.
Then the optimal x given by $x^* = y/\|y\|$ if y is non-zero.
For $x = \mathbf{v}_k$ and $y = \sum_{l=1, l \neq k}^{K} c_{kl} \theta_{kl} \mathbf{P}_k^\top \mathbf{P}_l \mathbf{u}_l$, we prove lemma 2. □

Proof of lemma 3.

(i) Evaluating the function φ_k defined in (13) respectively in $\bar{\mathbf{v}}_k$ and $\mathbf{u}_k$ as follows :

$$\begin{aligned}
\varphi_k(\bar{\mathbf{v}}_k) = \sum_{l=1, l \neq k}^{K} c_{kl} \theta_{kl} \bar{\mathbf{v}}_k^\top \mathbf{P}_k^\top \mathbf{P}_l u_l &= \bar{\mathbf{v}}_k^\top \mathbf{P}_k^\top \mathbf{P}_k \left(\sum_{l=1, l \neq k}^{K} c_{kl} \theta_{kl} \mathbf{P}_k^\top \mathbf{P}_l u_l \right) \\
&= \alpha_k \bar{\mathbf{v}}_k^\top \mathbf{P}_k^\top \mathbf{P}_k \bar{\mathbf{v}}_k \\
&= N \alpha_k cor\left(\mathbf{P}_k \bar{\mathbf{v}}_k, \mathbf{P}_k \bar{\mathbf{v}}_k \right) \\
&= N \alpha_k
\end{aligned}$$

and

$$\begin{aligned}
\varphi_k(\mathbf{u}_k) = \sum_{l=1, l \neq k}^{K} c_{kl} \theta_{kl} \mathbf{u}_k^\top \mathbf{P}_k^\top \mathbf{P}_l u_l &= \mathbf{u}_k^\top \mathbf{P}_k^\top \mathbf{P}_k \left(\sum_{l=1, l \neq k}^{K} c_{kl} \theta_{kl} \mathbf{P}_k^\top \mathbf{P}_l u_l \right) \\
&= \alpha_k \mathbf{u}_k^\top \mathbf{P}_k^\top \mathbf{P}_k \bar{\mathbf{v}}_k \\
&= N \alpha_k cor\left(\mathbf{P}_k u_k, \mathbf{P}_k \bar{\mathbf{v}}_k \right)
\end{aligned}$$

it follows that

$$2\left[\varphi_k(\bar{\mathbf{v}}_k) - \varphi_k(\mathbf{u}_k)\right] = N \alpha_k \left[2 - 2cor\left(\mathbf{P}_k \mathbf{u}_k, \mathbf{P}_k \bar{\mathbf{v}}_k\right)\right] = \alpha_k \left\| \mathbf{P}_k \bar{\mathbf{v}}_k - \mathbf{P}_k \mathbf{u}_k \right\|^2 \tag{16}$$

Considering the following equalities :

$$\begin{aligned}
\rho\left(\bar{\mathbf{v}}_1, \mathbf{u}_2, \ldots, \mathbf{u}_K\right) - \rho\left(\mathbf{u}_1, \mathbf{u}_2, \ldots, \mathbf{u}_K\right) &= 2\left[\varphi_1\left(\bar{\mathbf{v}}_1\right) - \varphi_1\left(\mathbf{u}_1\right)\right] \\
\rho\left(\bar{\mathbf{v}}_1, \bar{\mathbf{v}}_2, \ldots, \mathbf{u}_K\right) - \rho\left(\bar{\mathbf{v}}_1, \mathbf{u}_2, \ldots, \mathbf{u}_K\right) &= 2\left[\varphi_2\left(\bar{\mathbf{v}}_2\right) - \varphi_2\left(\mathbf{u}_2\right)\right] \\
&\ldots \\
\rho\left(\bar{\mathbf{v}}_1, \bar{\mathbf{v}}_2, \ldots, \bar{\mathbf{v}}_K\right) - \rho\left(\bar{\mathbf{v}}_1, \bar{\mathbf{v}}_2, \ldots, \bar{\mathbf{v}}_{K-1}, \mathbf{u}_K\right) &= 2\left[\varphi_K\left(\bar{\mathbf{v}}_K\right) - \varphi_K\left(\mathbf{u}_K\right)\right],
\end{aligned}$$

and summing over k, it follows

$$\rho\left(\bar{\mathbf{v}}_1, \bar{\mathbf{v}}_2, \ldots, \bar{\mathbf{v}}_K\right) - \rho\left(\mathbf{u}_1, \mathbf{u}_2, \ldots, \mathbf{u}_K\right) = 2\sum_{k=1}^{K}\left[\varphi_k\left(\bar{\mathbf{v}}_k\right) - \varphi_k\left(\mathbf{u}_k\right)\right] \tag{17}$$

Substitution (16) in the right of the equality (17) gives :

$$\rho\big(\bar{\mathbf{v}}_1, \bar{\mathbf{v}}_2, \cdots, \bar{\mathbf{v}}_K\big) - \rho\big(\mathbf{u}_1, \mathbf{u}_2, \cdots, \mathbf{u}_K\big) = 2\Bigg(\sum_{k=1}^{K}\big(\varphi_k\big(\bar{\mathbf{v}}_k\big) - \varphi_k\big(\mathbf{u}_k\big)\Big) = \sum_{k=1}^{K}\alpha_k \left\|\mathbf{P}_k\bar{\mathbf{v}}_k - \mathbf{P}_k\mathbf{u}_k\right\|^2.$$

□

Declarations

Conflict of interest The authors have no conflicts of interest to declare that are relevant to the content of this article.

Acknowledgment

The authors gratefully acknowledge the support of editors during the publication process as well as the useful feedback provided by two anonymous referees.

References

[1] E. Ciavolino, J.-H. Cheah, and B. Simonetti, *Introduction to advanced partial least squares path modeling*, Quality & Quantity, vol. 57, no. Suppl 4, pp. 517–520, 2023.

[2] S. Dray and A. Siberchicot, *Package 'ade4'*, Université de Lyon, Lyon, France, 2017.

[3] M. Hanafi, *PLS path modelling: computation of latent variables with the estimation mode B*, Computational Statistics, vol. 22, no. 2, pp. 275–292, 2007.

[4] M. Hanafi, P. Dolce, and Z. El Hadri, *Generalized properties for Hanafi-Wold's procedure in partial least squares path modeling*, Computational Statistics, vol. 36, pp. 603–614, 2021. https://doi.org/10.1007/s00180-020-01015-w

[5] M. Hanafi, Z. El Hadri, A. Sahli, and P. Dolce, *Overcoming convergence problems in PLS path modelling*, Computational Statistics, vol. 37, no. 5, pp. 2437–2470, 2022. https://doi.org/10.1007/s00180-022-01204-9

[6] J. Henseler, *On the convergence of the partial least squares path modeling algorithm*, Computational Statistics, vol. 25, no. 1, pp. 107–120, 2010. https://doi.org/10.1007/s00180-009-0164-x

[7] K. G. Jöreskog, *A general method for the analysis of covariance structure*, Biometrika, vol. 57, pp. 239–251, 1970.

[8] H. Latan, J. F. Hair Jr, R. Noonan, and M. Sabol, *Introduction to the partial least squares path modeling: Basic concepts and recent methodological enhancements*, in *Partial Least Squares Path Modeling: Basic Concepts, Methodological Issues and Applications*, Springer, 2023, pp. 3–21.
(2013). Package 'semPLS'.

[9] A.Monecke, M. A.Monecke, and X. M. L Suggests, *Package 'semPLS'*,2013, Citeseer

[10] S. Petter, and Y. Hadavi, *Use of partial least squares path modeling within and across business disciplines*, in *Partial Least Squares Path Modeling: Basic Concepts, Methodological Issues and Applications*, Springer, 2023, pp. 55–79.

[11] G. Sanchez and L. Trinchera, *Package 'plspm'*, Citeseer: State College, PA, USA, 2013.

[12] A. K. Smilde, T. Næs, and K. H. Liland, *Multiblock data fusion in statistics and machine learning: Applications in the natural and life sciences*, John Wiley & Sons, 2022.

[13] A. Tenenhaus, V. Guillemot, and A. Tenenhaus, *Package 'RGCCA'*, Available online: GitHub-BrainAndSpine Institute/rgcca_Rpackage (accessed on 10-03-2021), Citeseer, 2017.

[14] M. Tenenhaus, and V.E. Vinzi, and Y.M. Chatelin, and C.Lauro, *PLS path modeling*, Computational statistics & data analysis, Elsevier, 2005, vol. 48, no. 1, pp 159-205.

[15] S. Venturini, M. Mehmetoglu, and H. Latan, *Software packages for partial least squares structural equation modeling: An updated review*, in *Partial Least Squares Path Modeling: Basic Concepts, Methodological Issues and Applications*, Springer, 2023, pp. 113–152.

[16] H. Wold, *Soft modelling: The basic design and some extensions*, in *Systems under indirect observation*, vol. 2, K. G. Jöreskog and H. Wold (Eds.), North Holland, Amsterdam, pp. 1–54, 1982.

[17] H. Wold, *Partial least squares*, in *Encyclopaedia of Statistical Sciences*, vol. 6, S. Kotz and N. L. Johnson (Eds.), John Wiley Sons, New York, pp. 581–591, 1985.

[18] P. XLSTAT Addinsoft, *Data analysis and statistical solution for Microsoft Excel*, Paris: Addinsoft SARL, 2021.